

Fermi-liquid and Fermi-surface-geometry effects in the propagation of low-frequency electromagnetic waves through thin metal films

Natalya A. Zimbovskaya

Department of Physics and Electronics, University of Puerto Rico, Humacao, Puerto Rico 00791

(Received 17 April 2007; published 8 August 2007)

In the present work, we theoretically analyze the contribution from a transverse Fermi-liquid collective mode to the transmission of electromagnetic waves through a thin film of a clean metal in the presence of a strong external magnetic field. We show that at the appropriate Fermi surface geometry, the transverse Fermi-liquid wave may appear in conduction electron liquid at frequencies ω significantly smaller than the cyclotron frequency of charge carriers, Ω , provided that the mean collision frequency τ^{-1} is smaller than ω . Also, we show that in realistic metals, size oscillations in the transmission coefficient associated with the Fermi-liquid mode may be observable in experiments. Under certain conditions, these oscillations may predominate over the remaining size effects in the transmission coefficient.

DOI: [10.1103/PhysRevB.76.075104](https://doi.org/10.1103/PhysRevB.76.075104)

PACS number(s): 71.18.+y

I. INTRODUCTION

It is well known that electromagnetic waves incident on the surface of a metal cannot penetrate inside the metal deeper than a thin surface layer (skin layer). This happens due to the damping effect of conduction electrons absorbing the wave energy via dissipationless Landau damping mechanism.¹ A strong magnetic field $\mathbf{B}=(0,0,B)$ applied to the metal restricts the motion of electrons in the x,y plane, creating “windows of transparency.” These windows are regions in the q,ω plane (q,ω are the wave vector and the frequency of the electromagnetic wave, respectively) where the Landau damping cannot take place. As a result, in the presence of the external magnetic field, various weakly attenuating electromagnetic waves, such as helicoidal, cyclotron, and magnetohydrodynamic waves, may propagate in the electron liquid of a metal.^{2,3}

Fermi-liquid (FL) correlations of conduction electrons bring changes in the wave spectra. Also, new collective modes may appear in metals due to FL interactions among the electrons. These modes solely occur owing to the FL interactions, so they are absent in a gas of charge carriers. Among these modes, there is the Fermi-liquid cyclotron wave first predicted by Silin⁴ and observed in alkali metals.^{5,6} In a metal with the nearly spherical Fermi surface (FS), this mode is the transverse circularly polarized wave propagating along the external magnetic field whose dispersion within the collisionless limit ($\tau \rightarrow \infty$) has the form⁷

$$\frac{\omega}{\omega_0} = 1 + \frac{8}{35} \frac{1}{\alpha} (qR)^2. \quad (1)$$

Here, $R=v_0/\Omega$; v_0 is the maximum value of the electron velocity component along the magnetic field (for the spherical FS, v_0 equals the Fermi velocity v_F); $\Omega=eB/mc$ is the cyclotron frequency, τ is the electron scattering time, and the dimensionless parameter α characterizes FL interactions of conduction electrons. For the spherical FS, the electron cyclotron mass coincides with their effective mass m . The difference between the frequency $\omega_0=\omega(0)$ and the cyclotron frequency is determined with the value of the Fermi-liquid parameter α , namely, $\omega_0=\Omega(1+\alpha)$. Depending on whether α

takes on a positive or negative value, ω_0 is greater for smaller than Ω . Further, we assume for certainty that $\alpha < 0$. When $qR \ll 1$, the dispersion curve of this Fermi-liquid cyclotron wave is situated in the window of transparency whose boundary is given by the relation $\omega=\Omega-qv_0$, which corresponds to the Doppler-shifted cyclotron resonance for the conduction electrons.

This is shown in Fig. 1 (left panel). However, the dispersion curve meets the boundary of the transparency region at $q=q_m \approx 5|\alpha|/3R$,⁷ and at this value of q , the dispersion curve is terminated.⁸ So, for reasonably weak FL interactions ($|\alpha| \sim 0.1$), the Fermi-liquid cyclotron wave may appear only at $qR \ll 1$ and its frequency remains close to the cyclotron frequency for the whole spectrum.⁹ Similar conclusions were made using some other models to mimic the FS shape such as an ellipsoid, a nearly ellipsoidal surface, and a lens made out of two spherical segments.^{10,11}

It is clear that the main contribution to the formation of a weakly attenuated collective mode near the boundary of the transparency region at $\omega \ll \Omega$ comes from those electrons

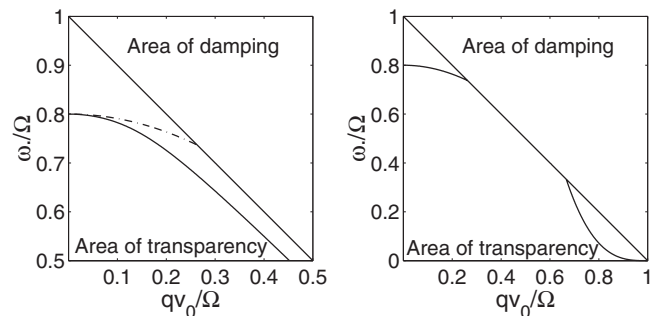


FIG. 1. Left panel: Dispersion of the transverse Fermi-liquid cyclotron wave traveling along the external magnetic field for the spherical (dash-dot line) and paraboloidal (solid line) FSs. The curves are plotted using Eqs. (1) and (3) assuming $\alpha=-0.2$. Right panel: A schematic plot of the dispersion of a transverse Fermi-liquid mode in a metal whose FS includes nearly paraboloidal segments. The low-frequency ($\omega \ll \Omega$) branch is shown along with the cyclotron wave. For both panels, the straight line corresponds to the Doppler-shifted cyclotron resonance.

which move with the greatest possible speed along the magnetic field \mathbf{B} . The greater is the relative number of such electrons, the more favorable conditions are developing for the wave to emerge and to exist at comparatively low frequencies, $\tau^{-1} \ll \omega \ll \Omega$. The relative number of such “efficient” electrons is determined with the FS shape, and the best conditions are reached when the FS includes a lens made out of two paraboloidal cups. Such lens corresponds to the following energy-momentum relation for the relevant conduction electrons:

$$E(\mathbf{p}) = \frac{\mathbf{p}_\perp^2}{2m_\perp} + v_0|p_z|, \quad (2)$$

where p_z, \mathbf{p}_\perp are the electron quasimomentum components in the plane perpendicular to the external magnetic field $\mathbf{B} = (0, 0, B)$ and along the magnetic field, respectively. The effective mass m_\perp corresponds to electron motions in the x, y plane. This model was employed in some earlier works to study transverse collective modes occurring in a gas of charge carriers near the Doppler-shifted cyclotron resonance which are known as dopplersons.^{12–14} It was shown¹⁵ that for negative values of the Fermi-liquid parameter α and provided that the FS contains a paraboloidal segment described by Eq. (2), the dispersion of the transverse Fermi-liquid wave propagating along the magnetic field has the form ($\tau \rightarrow \infty$)

$$\frac{\omega}{\Omega} = 1 - \frac{1}{2}(qR + |\alpha|) - \frac{1}{2} \sqrt{(qR - |\alpha|)^2 + \frac{4}{3} \frac{|\alpha|(qR)^2}{qR + \sqrt{(qR)^2 + |\alpha|^2}}}, \quad (3)$$

where $\Omega = eB/m_\perp c$. This result shows that for the paraboloidal FS, there are no limitations on frequency of the Fermi-liquid cyclotron wave within the collisionless limit (see Fig. 1, left panel). The only restriction on the wave frequency is caused by the increase of the wave attenuation due to collisions. Taking into account electron scattering, one can prove that the wave is weakly attenuated up to a magnitude of the wave vector of the order of $\Omega(1 - 1/|\alpha|\Omega\tau)/v_0$. This value (especially for small $|\alpha|$) is significantly larger than the value q_m for the spherical Fermi surface. Therefore, the frequency of the Fermi-liquid cyclotron waves for negative α can be much smaller than Ω (remaining greater than $1/\tau$). Comparing the dispersion curves of the transverse Fermi-liquid cyclotron wave for spherical and paraboloidal FSs, we see that the FS geometry strongly affects the wave spectrum, and it may provide a weak attenuation of this mode at moderately low frequencies, $\omega \ll \Omega$. In the present work, we concentrate on the analysis of the effects of the FS geometry on the occurrence of weakly damped Fermi-liquid cyclotron waves propagating in metals along the applied magnetic field at low frequencies ($\tau^{-1} \ll \omega \ll \Omega$).

We show below that in realistic metals with appropriate FSs, one may expect a low-frequency Fermi-liquid mode to occur along with the Fermi-liquid cyclotron wave, as presented in Fig. 1 (right panel). Both waves have the same polarization and travel in the same direction. Also, we con-

sider possible manifestations of these low-frequency Fermi-liquid waves by estimating the magnitude of the corresponding size oscillations in the transmission coefficient for electromagnetic waves propagating through a thin metal film.

II. DISPERSION EQUATION FOR THE TRANSVERSE FERMILIQUID WAVES

In the following analysis, we restrict our consideration with the case of an axially symmetric Fermi surface whose symmetry axis is parallel to the magnetic field. Then, the response of the electron liquid of the metal to an electromagnetic disturbance could be expressed in terms of the electron conductivity circular components, $\sigma_\pm(\omega, \mathbf{q}) = \sigma_{xx}(\omega, \mathbf{q}) \pm i\sigma_{yx}(\omega, \mathbf{q})$. The above restriction on the FS shape enables us to analytically calculate the conductivity components. Also, the recent analysis carried out in Ref. 16 showed that no qualitative difference was revealed in the expressions for the principal terms of the surface impedance computed for the axially symmetric FSs and those not possessing such symmetry, provided that \mathbf{B} is directed along a high order symmetry axis of the Fermi surface. This gives grounds to expect the currently employed model to catch main features in the electronic response which remain exhibited when the FSs of generalized (nonaxially symmetric) shape are taken into consideration.

Within the phenomenological Fermi-liquid theory, electron-electron interactions are represented by a self-consistent field affecting any single electron included in the electron liquid. Due to this field, the electron energies $E(\mathbf{p})$ get renormalized, and the renormalization corrections depend on the electron position \mathbf{r} and time t :

$$\Delta E = \text{Tr}_{\sigma'} \int \frac{d^3 \mathbf{p}'}{(2\pi\hbar)^3} F(\mathbf{p}, \hat{\sigma}; \mathbf{p}', \hat{\sigma}') \delta\rho(\mathbf{p}', \mathbf{r}, \hat{\sigma}', t). \quad (4)$$

Here, $\delta\rho(\mathbf{p}, \mathbf{r}, \hat{\sigma}, t)$ is the electron density matrix, \mathbf{p} is the electron quasimomentum, and $\hat{\sigma}$ is the spin Pauli matrix. The trace is taken over spin numbers σ . The Fermi-liquid kernel included in Eq. (4) is known to have the form

$$F(\mathbf{p}, \hat{\sigma}; \mathbf{p}', \hat{\sigma}') = \varphi(\mathbf{p}, \mathbf{p}') + 4(\hat{\sigma}\hat{\sigma}')\psi(\mathbf{p}, \mathbf{p}'). \quad (5)$$

For an axially symmetric FS, the functions $\varphi(\mathbf{p}, \mathbf{p}')$ and $\psi(\mathbf{p}, \mathbf{p}')$ do not vary under identical change in the directions of projections \mathbf{p}_\perp and \mathbf{p}'_\perp . These functions actually depend only on the cosine of the angle θ between the vectors \mathbf{p}_\perp and \mathbf{p}'_\perp and on the longitudinal components of the quasimomenta, p_z and p'_z .

We can separate out even and odd in the $\cos \theta$ parts of the Fermi-liquid functions. Then, the function $\varphi(\mathbf{p}, \mathbf{p}')$ can be presented as follows:

$$\varphi(\mathbf{p}, \mathbf{p}') = \varphi_0(p_z, p'_z, \cos \theta) + (\mathbf{p}_\perp \mathbf{p}'_\perp) \varphi_1(p_z, p'_z, \cos \theta), \quad (6)$$

where φ_0, φ_1 are even functions of $\cos \theta$. Due to invariance of the FS under the replacements $\mathbf{p} \rightarrow -\mathbf{p}$ and $\mathbf{p}' \rightarrow -\mathbf{p}'$, the functions φ_0 and φ_1 should not vary under simultaneous change in signs of p_z and p'_z . Using this, we can subdivide the functions φ_0, φ_1 into the parts which are even and odd in p_z, p'_z , and to rewrite Eq. (6) as

$$\varphi(p_z, p'_z, \cos \theta) = \varphi_{00} + p_z p'_z \varphi_{01} + (\mathbf{p}_\perp \mathbf{p}'_\perp)(\varphi_{10} + p_z p'_z \varphi_{11}). \quad (7)$$

The function $\psi(\mathbf{p}, \mathbf{p}')$ may be presented in the same way. In Eq. (7), the functions $\varphi_{00}, \varphi_{01}, \varphi_{10}, \varphi_{11}$ are even in all their arguments, namely, p_z, p'_z , and $\cos \theta$.

In the following computation of the electron conductivity, we employ the linearized transport equation for the nonequilibrium distribution function $g(\mathbf{p}, \mathbf{r}, t) = \text{Tr}_\sigma[\delta\rho(\mathbf{p}, \mathbf{r}, \hat{\sigma}, t)]$. While considering a simple harmonic disturbance, $\mathbf{E} = \mathbf{E}_{q\omega} \exp(i\mathbf{q} \cdot \mathbf{r} - i\omega t)$, we may represent the coordinate and space dependencies of the distribution function $g(\mathbf{p}, \mathbf{r}, t)$ as $g(\mathbf{p}, \mathbf{r}, t) = g_{q\omega} \exp(i\mathbf{q}\mathbf{r} - i\omega t)$. Then, the linearized transport equation for the amplitude $g_{q\omega}(\mathbf{p})$ takes on the form

$$\frac{\partial g_{q\omega}^e}{\partial \tilde{t}} + i\mathbf{q} \cdot \mathbf{v} g_{q\omega}^e + \left(\frac{1}{\tau} - i\omega \right) g_{q\omega}^e + e \frac{\partial f_{\mathbf{p}}}{\partial E_{\mathbf{p}}} \mathbf{v} \mathbf{E}_{q\omega} = 0. \quad (8)$$

Here, $f_{\mathbf{p}}$ is the Fermi distribution function for the electrons with energies $E(\mathbf{p})$, and $\mathbf{v} = \partial E / \partial \mathbf{p}$ is the electron velocity. The collision term in Eq. (8) is written using the τ approximation which is acceptable for high frequency disturbances ($\omega\tau \gg 1$) considered in the present work. The derivative $\partial g_{q\omega}^e / \partial \tilde{t}$ is to be taken over the variable \tilde{t} which has the meaning of time of the electron motion along the cyclotron orbit. The function $g_{q\omega}^e(\mathbf{p})$ introduced in Eq. (8) is related to $g_{q\omega}(\mathbf{p})$ as follows:

$$g_{q\omega}^e(\mathbf{p}) = g_{q\omega}(\mathbf{p}) - \frac{\partial f_{\mathbf{p}}}{\partial E_{\mathbf{p}}} \sum_{\mathbf{p}'} \varphi(\mathbf{p}, \mathbf{p}') g_{q\omega}(\mathbf{p}'). \quad (9)$$

So, the difference between the distribution functions $g_{q\omega}(\mathbf{p})$ and $g_{q\omega}^e(\mathbf{p})$ originates from the FL interactions in the system of conduction electrons.

Using the transport equation [Eq. (8)], one may derive the expressions for $\sigma_{\pm}(\omega, \mathbf{q})$ including terms originating from the Fermi-liquid interactions. The computational details are given in Refs. 17 and 18. The results for the circular components of the conductivity for a singly connected FS can be written as follows:

$$\sigma_{\pm} = \frac{2ie^2 A(0)}{(2\pi\hbar)^3 q} \times \frac{\left[\Phi_0^{\pm} \left(1 - \frac{\alpha_2 u}{Q_2} \Phi_2^{\pm} \right) + \frac{\alpha_2 u}{Q_2} (\Phi_1^{\pm})^2 \right]}{\left[\left(1 - \frac{\alpha_1 u}{Q_0} \Phi_0^{\pm} \right) \left(1 - \frac{\alpha_2 u}{Q_2} \Phi_2^{\pm} \right) + \frac{\alpha_1 \alpha_2}{Q_0 Q_2} u^2 (\Phi_1^{\pm})^2 \right]}. \quad (10)$$

Here,

$$\Phi_n^{\pm} = \int_{-1}^1 \frac{\bar{a}(x) \bar{m}_{\perp}(x) x^n dx}{u \chi_{\pm} \mp \bar{v}(x)}, \quad (11)$$

$$Q_n = \int_{-1}^1 \bar{a}(x) \bar{m}_{\perp}(x) x^n dx. \quad (12)$$

$$\bar{a}(x) = A(x)/A(0), \quad \bar{v}(x) = v_z/v_0,$$

$$\bar{m}_{\perp}(x) = m_{\perp}(x)/m_{\perp}(0), \quad x = p_z/p_0,$$

$$\chi_{\pm} = 1 \pm \Omega/\omega + i/\omega\tau, \quad u = \omega/qv_0, \quad (13)$$

where v_0, p_0 are the maximum values of the longitudinal components of the electron quasimomentum and velocity; $A(x)$ is the FS cross-sectional area; $m_{\perp}(x)$ is the cyclotron mass of electrons. The dimensionless factors $\alpha_{1,2}$ in Eq. (10) are related to the Fermi-liquid parameters φ_{10} and φ_{11} :

$$\alpha_{1,2} = f_{1,2}/(1 + f_{1,2}), \quad (14)$$

where

$$f_1 = \frac{2}{(2\pi\hbar)^3} \int p_{\perp}^2 \varphi_{10} m_{\perp} dp_z, \quad (15)$$

$$f_2 = \frac{2}{(2\pi\hbar)^3} \int p_{\perp}^2 p_z^2 \varphi_{11} m_{\perp} dp_z.$$

When an external magnetic field is applied, electromagnetic waves may travel inside the metal. In the present work, we are interested in the transverse waves propagating along the magnetic field. The corresponding dispersion equation has the form

$$c^2 q^2 - 4\pi i \omega \sigma_{\pm}(\omega, \mathbf{q}) = 0. \quad (16)$$

When dealing with the electron Fermi liquid, this equation for “-” polarization has solutions corresponding to helicoidal waves and the transverse Fermi-liquid waves traveling along the magnetic field, while when the relevant charge carriers are holes, the “+” polarization is to be chosen in Eq. (16).

Considering these waves, we may simplify the dispersion equation [Eq. (16)] by omitting the first term. Also, we can neglect corrections of the order of $c^2 q^2 / \omega_p^2$ (ω_p is the electron plasma frequency) in the expression for the conductivity. Then the Fermi-liquid parameter α_1 falls out from the dispersion equation, and the latter takes on the form

$$\Delta(u) = 1/\alpha_2, \quad (17)$$

where $\Delta(u) = (u/Q_2)[\Phi_2^- - (\Phi_1^-)^2 / \Phi_0^-]$.

Assuming the mass m_{\perp} to be the same over the whole FS and expanding the integrals Φ_n^- in powers of u^{-1} and keeping terms of the order of u^{-2} , we get the dispersion relation for the cyclotron mode at small $q(u \gg 1)$:

$$\omega = \Omega(1 + f_2) \left[1 + \frac{\eta}{f_2} \left(\frac{qv_0}{\Omega} \right)^2 \right], \quad (18)$$

where

$$\eta = \left\{ \int_{-1}^1 \bar{a}(x) \bar{v}^2(x) x^2 dx - \frac{1}{Q_0} \left[\int_{-1}^1 \bar{a}(x) \bar{v}(x) x dx \right]^2 \right\} \frac{1}{Q_2}. \quad (19)$$

For an isotropic electron liquid, $\eta = 8/35$, and expression (18) coincides with expression (1) where $\alpha = f_2$. Also, adopt-

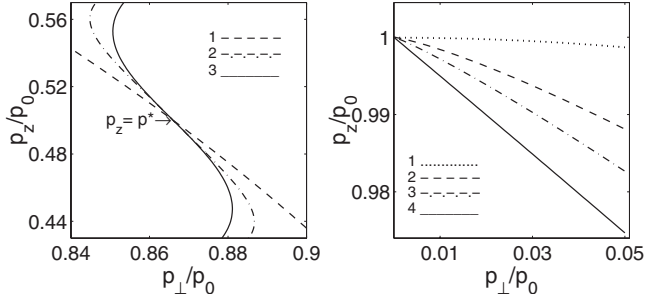


FIG. 2. Schematic plots of the FS profiles in the vicinities of inflection lines (left panel) and vertices (right panel). Left panel: The profiles are drawn in accordance with Eq. (23) assuming $p^* = 0.5p_0$, $|d^s \bar{a}/dx^s|_{x=x^*} = |d\bar{a}/dx|_{x=x^*} = 1$, and $s=5$ (curve 2) and $s=3$ (curve 3). Curve 1 corresponds to a paraboloidal strip on the FS near $x^* = 0.5(s \rightarrow \infty)$. Right panel: The curves are plotted assuming $x^* = 1$ and $\bar{a}(1) = 0$. Curves 1 and 4 correspond to spherical and paraboloidal FSs, respectively; curves 2 and 3 represent nearly paraboloidal FSs with $s=7$ and 9 , respectively.

ing model (2), we may analytically calculate the integrals Φ_n^- and transform the dispersion equation [Eq. (17)] as

$$3(\chi_- + \alpha_2)[1 - (u\chi_-)^2] = \alpha_2. \quad (20)$$

At small negative values of the parameter α_2 , this equation has a solution of the form in Eq. (3) where $\alpha = \alpha_2$.

Now, we start to analyze possibilities for the low-frequency ($\tau^{-1} \ll \omega \ll \Omega$) transverse Fermi-liquid mode to emerge in realistic metals where the cyclotron mass depends on p_z . Such waves could appear near the Doppler-shifted cyclotron resonance. Assuming $\alpha_2 < 0$, we may describe the relevant boundary of the transparency region by the equations

$$S(\omega, q, p_z) = 0, \quad (21)$$

$$\partial S(\omega, q, p_z) / \partial p_z = 0,$$

where $S(\omega, q, p_z) = \omega - \Omega(p_z) + qv_z(p_z)$. For small ω , we have

$$\Omega(p_z) \left(1 + \frac{cq}{2\pi|e|B} \frac{dA}{dp_z} \right) = 0, \quad (22)$$

$$\frac{d\Omega}{dp_z} \left(1 + \frac{cq}{2\pi|e|B} \frac{dA}{dp_z} \right) + \frac{\Omega(p_z)cq}{2\pi|e|B} \frac{d^2A}{dp_z^2} = 0.$$

We see that the attenuation at the boundary for small ω is carried out by the electrons belonging to neighborhoods of particular cross sections on the Fermi surface where extrema of the value dA/dp_z are reached. These can be neighborhoods of limiting points or lines of inflection, as shown in Fig. 2.

In general, to study the various effects in the response of an electron liquid of a metal near the Doppler-shifted cyclotron resonance, one must take into account contributions from all segments of the FS, therefore, the expressions for the conductivity components [Eq. (10)] are to be correspondingly generalized. However, in studies of our problem, it is possible to separate out that particular segment of the FS where the electrons producing the low-frequency Fermi-

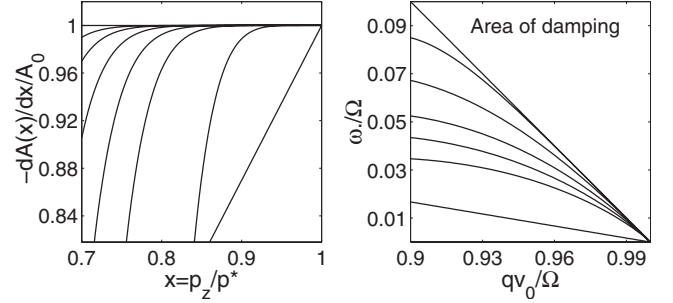


FIG. 3. Left panel: Dependencies of $d\bar{a}/dx$ of x near the inflection line on the FS at $x=x^*$. The curves are plotted for $s = 4, 5, 6, 7, 8, 9$ (from the right to the left). Right panel: Dispersion curves of the low-frequency transverse Fermi-liquid waves. The curves are plotted at $\alpha_2 = -0.2$; $s = 4, 5, 6, 7, 8$ and $s \rightarrow \infty$ (from the top to the bottom) in the collisionless limit assuming that $|d^s \bar{a}/dx^s|_{x=x^*} = |d\bar{a}/dx|_{x=x^*} = 1$.

liquid wave belong. The contribution from the rest of the FS is small, and we can omit it, as shown in Ref. 15.

So, in the following studies, we may use the dispersion equation [Eq. (17)] where the integrals Φ_n^\pm are calculated for the appropriate segment of the FS. It follows from this equation that the dispersion curve of the cyclotron wave will not intersect the boundary of the region of transparency when the function $\Delta(u)$ diverges there. A similar analysis was carried out in the theory of dopplersons.¹⁴ It was proven that when the appropriate component of the conductivity [integral of a type of $\Phi_0(u)$] goes to infinity at the Doppler-shifted cyclotron resonance, it provides the propagation of the dopplerson without damping in a broad frequency range.

In the further analysis, we assume for certainty that the extrema of dA/dp_z are reached at the inflection lines $p_z = \pm p^*$. In the vicinities of these lines, we can use the following approximation:

$$\bar{a}(x) \approx \bar{a}(x^*) + \frac{d\bar{a}}{dx} \Big|_{x=x^*} (x \mp x^*) \pm \frac{1}{s!} \frac{d^s \bar{a}}{dx^s} \Big|_{x=x^*} (x \mp x^*)^s. \quad (23)$$

In this expression, $x^* = p_z/p^*$, and the parameter $s (s \geq 3)$ characterizes the FS shape near the inflection lines at $x = \pm x^*$. The greater is the value of s , the closer is the FS near $p_z = \pm p^*$ to a paraboloid (see Fig. 2). When $s=1$, the FS has spherical or ellipsoidal shape in the vicinities of these points.

The dependencies of the derivative $d\bar{a}/dx$ of x near $x = x^*$ are presented in the left panel of Fig. 3. In this figure, the horizontal line corresponds to a paraboloidal FS ($s \rightarrow \infty$), the straight line on the right is associated with a spherical FS ($s=1$), and the remaining curves are plotted for ($s > 3$). We can see that the greater is the shape parameter s , the broader are the nearly paraboloidal strips in the vicinities of the FS inflection lines. Consequently, the greater number of conduction electrons is associated with the nearly paraboloidal parts of the FS, and this creates more favorable conditions for the wave to occur. A similar analysis may be carried out for the case when dA/dp_z reaches its extremal values at the vertices

of the FS. Again, to provide the emergence of the transverse low-frequency Fermi-liquid mode, the FS near $p_z = \pm p_0$ must be nearly paraboloidal in shape.

Using the asymptotic expression in Eq. (23), we may calculate the main term in the function $\Delta(u)$. This term diverges at the boundary of the region of transparency when $s \geq 3$, and it has the form

$$\Delta_-(u) = -\nu_s u (1 - u\chi_-)^{\mu_s} \quad (24)$$

where $\mu_s = (5 - 2s)/(2s - 2)$. For $s > 3$, μ_s takes on negative values, so within the collisionless limit ($\tau \rightarrow \infty$), the function $\Delta_-(u)$ diverges when $1 - u\chi_- \rightarrow 0$. The value of the factor ν_s is determined with the FS geometry near the inflection line, namely,

$$\nu_s = \frac{\pi \bar{a}(x^*) \bar{m}_\perp(x^*) \zeta_s}{Q_2(s-1) \sin[3\pi/(2s-2)]}, \quad (25)$$

where

$$\zeta_s = \left[\frac{|d^s \bar{a}/dx^s|_{x=x^*}}{(s-1)! |d\bar{a}/dx|_{x=x^*}} \right]^{-3/2(s-1)}. \quad (26)$$

Now, we can employ approximation (24) to solve the dispersion equation [Eq. (17)]. The solutions of this equation within the collisionless limit describing the low-frequency transverse Fermi-liquid wave at different values of the shape parameter s are plotted in Fig. 3 (right panel). All dispersion curves are located in between the boundary of the transparency window and the straight line corresponding to the limit $s \rightarrow \infty$ (a paraboloidal FS). The greater is the value of s , the closer is the dispersion curve to this line.

So, we showed that the low-frequency ($\omega \ll \Omega$) transverse Fermi-liquid wave could appear in a metal put into a strong ($\Omega\tau \gg 1$) magnetic field. This could happen when the FS is close to a paraboloid near those cross sections where dA/dp_z reaches its maxima or minima. Therefore, the possibility for this wave to propagate in a metal is provided with the local geometry of the Fermi surface near its inflection lines or vertices.

When Ω depends on p_z and ω increases, electrons associated with various cross sections of the Fermi surface participate in the formation of the wave. To provide the divergence of the function $\Delta(u)$ near the Doppler-shifted cyclotron resonance, we have to require that not merely narrow strips near lines of inflection or vicinities of limiting points but rather large segments of the Fermi surface be nearly paraboloidal. This condition is too stringent for FSs of real metals. So, we can expect that the dispersion curve of the low-frequency transverse Fermi-liquid wave intersects the boundary of the region of transparency at rather small ω , as shown in the right panel of Fig. 1.

III. SIZE OSCILLATIONS IN THE SURFACE IMPEDANCE

To clarify possible manifestations of the considered Fermi-liquid wave in experiments, we calculate the contribution of these waves to the transmission coefficient of a metal film. We assume that the film occupies the region $0 \ll z \leq L$ in

the presence of an applied magnetic field directed along a normal to the interfaces. An incident electromagnetic wave with the electric and magnetic components $\mathbf{E}(z)$ and $\mathbf{b}(z)$ propagates along the normal to the film. Also, we assume that the symmetry axis of the FS is parallel to the magnetic field (z axis) and the interfaces reflect the conduction electrons in a similar manner. Then, the Maxwell equations inside the metal are reduced to the couple of independent equations for circular components of the electrical field $E_\pm(z) \exp(-i\omega t)$ where ($E_\pm = E_x \pm iE_y$):

$$\frac{\partial^2 E_\pm}{\partial z^2} = -\frac{\omega^2}{c^2} E_\pm(z) - \frac{4\pi i \omega}{c^2} j_\pm(z), \quad (27)$$

$$\frac{\partial E_\pm(z)}{\partial z} = \mp \frac{\omega}{c} b_\pm(z). \quad (28)$$

Here, $b_\pm(z)$ and $j_\pm(z)$ are the magnitudes of the magnetic component of the incident electromagnetic wave and the electric current density inside the film, respectively. Expanding the magnitudes $E_\pm(z)$ and $j_\pm(z)$ in Fourier series, we arrive at the following equation for the Fourier transforms:

$$-\frac{c^2 q_n^2}{4\pi i \omega} E_n^\pm + j_n^\pm = \mp \frac{ic}{4\pi} [(-1)^n b_\pm(L) - b_\pm(0)], \quad (29)$$

where E_n^\pm equals

$$E_n^\pm = \int_0^L E_\pm(z) \cos(q_n z) dz \quad (30)$$

and $q_n = \pi n/L$.

It was mentioned above that possible frequencies of the low-frequency Fermi-liquid mode have to satisfy the inequality $(|\alpha_2| \tau)^{-1} \ll \omega < \Omega$. For $\tau < 10^{-9}$ s, the frequency ω cannot be lower than $10^9 - 10^{10}$ s⁻¹. Due to the high density of conduction electrons in good metals, the skin depth δ may be very small. Assuming the electron density to be of the order of 10^{30} m⁻³ and the mean free path $l \sim 10^{-5}$ m (a clean metal), we estimate the skin depth at the disturbance frequency $\omega \sim 10^9$ s⁻¹ as $\delta \sim 10^{-6}$ m. Therefore, at high frequencies ω , the skin effect in good metals becomes extremely anomalous so that $\delta/l \sim 10^{-1} - 10^{-2}$ or even smaller. Correspondingly, the anomaly parameter $\xi = l/\omega\tau\delta$ is of the order $10^2 - 10^3$. Thus, for the whole frequency range of the considered Fermi-liquid mode, the skin effect is of anomalous character. Under these conditions, electrons must move nearly in parallel with the metal surface to remain in the skin layer for a sufficiently long while. The effect of the surface roughness on such electrons is rather small. Nevertheless, we may expect the effects of surface roughness to bring changes in the corresponding size oscillations of the transmission coefficient. To take into account the effects of diffuse scattering of electrons from the surfaces of the film, one must start from the following expression for the Fourier transforms of the current density components:

$$j_n^\pm = \sigma_n^\pm E_n^\pm + \sum_{n'=0} \left(1 - \frac{1}{2} \delta_{n'0}\right) \sigma_{nn'}^\pm E_{n'}^\pm, \quad (31)$$

where $\sigma_n^\pm = \sigma_{xx}(\omega, q_n) \pm i\sigma_{yx}(\omega, q_n)$ are the circular components of the bulk conductivity and $\sigma_{nn'}^\pm = \sigma_{xx}(\omega, q_n, q_{n'}) \pm i\sigma_{yx}(\omega, q_n, q_{n'})$ are the circular components of the surface conductivity. The effects originating from the surface roughness are included in $\sigma_{nn'}^\pm$, which becomes zero for a smooth surface providing the specular reflection of electrons. The calculation of $\sigma_{nn'}^\pm$ is a very difficult task which could hardly be carried out analytically if one takes into account Fermi-liquid correlations of electrons. However, such calculations were performed for a special case of paraboloidal FS corresponding to the energy-momentum relation [Eq. (2)] in the earlier work.¹⁹ As was mentioned before, the FS segments which give the major contributions to the formation of the transverse Fermi-liquid mode are nearly paraboloidal in shape, therefore, the results of the work¹⁹ may be used to qualitatively estimate the significance of the surface scattering of electrons under the conditions of the anomalous skin effect. We assume for simplicity that the diffuse scattering is characterized by a constant $P(0 < P < 1)$. When $P=0$, the reflection of electrons is purely specular, whereas $P=1$ corresponds to the completely diffuse reflection. Adopting expression (2) to describe the electron spectrum, one could obtain

$$\sigma_n^\pm = \pm \frac{iNe^2}{3m_\perp \omega} \chi_\pm \left[\frac{1}{\theta_n^\pm} + \frac{2(\chi_\pm^*/\chi_\pm)^2}{\theta_n^{\pm*}} \right], \quad (32)$$

$$\sigma_{nn'}^\pm = \frac{4}{3} \frac{Ne^2}{m_\perp \omega} \lambda \frac{v_0}{\omega L} \chi_\pm^2 \left[\frac{1}{1 \mp \lambda s_\pm} \frac{1}{\theta_n^{\pm*} \theta_{n'}^\pm} + \frac{2(\chi_\pm^*/\chi_\pm)^4}{1 \mp \lambda s_\pm \chi_\pm^*/\chi_\pm} \frac{1}{\theta_n^{\pm*} \theta_{n'}^{\pm*}} \right], \quad (33)$$

where N is the electron density,

$$s_\pm = i \tan(L\Omega \chi_\pm / v_0),$$

$$s_\pm^* = i \tan(L\Omega \chi_\pm^* / v_0),$$

$$\theta_n^\pm = \chi_\pm^2 - q_n^2,$$

$$\theta_n^{\pm*} = \chi_\pm^{*2} - q_n^2 \equiv \chi_\pm^2 \mp \alpha_2 \chi_\pm - q_n^2. \quad (34)$$

The parameter $\lambda = P/(2-P)$ characterizes the strength of the diffuse component in the electron scattering from the surfaces of the metal film.

Comparing expressions (32) and (33), we conclude that σ_n^\pm predominates over $\sigma_{nn'}^\pm$ in magnitude when $\lambda \xi \delta / L \ll \omega / \Omega$. Assuming that the anomaly parameter $\xi \sim 10^2$, the skin depth $\delta \sim 10^{-6}$ m, and $\omega \sim \Omega$, we conclude that the roughness of the surface does not affect the transmission coefficient if the film thickness L is not smaller than 10^{-4} m. For thinner films, the surface roughness may bring noticeable changes into the transmission. For instance, when $L \sim l \sim 10^{-5}$ m, we may neglect the diffuse contribution to the

electron reflection at the surfaces of the film when $\lambda < 0.1 (P < 0.2)$. In further calculations, we assume the film surfaces to be smooth enough, so that we could treat the electron reflection from the metal film surfaces as nearly specular. Correspondingly, we omit the second term in expression (31).

Substituting the resulting expressions for j_n^\pm into Eq. (29), we get

$$E_\pm^\pm = \mp \frac{\omega}{c} F_\pm(\omega, q_n) [(-1)^n b_\pm(L) - b_\pm(0)]. \quad (35)$$

Here, we introduced the notation

$$F_\pm(\omega, q_n) = \left(q_n^2 - \frac{4\pi i \omega}{c^2} \sigma_n^\pm \right)^{-1}. \quad (36)$$

Now, using these expressions for the Fourier transforms, we get the relations for the electric and magnetic fields at the interfaces $z=0$ and $z=L$:

$$E_\pm(0) = \frac{c}{4\pi} [Z_\pm^{(0)} b_\pm(0) - Z_\pm^{(1)} b_\pm(L)], \quad (37)$$

$$E_\pm(L) = \frac{c}{4\pi} [Z_\pm^{(1)} b_\pm(0) - Z_\pm^{(0)} b_\pm(L)], \quad (38)$$

where the surface impedances are given by

$$Z_\pm^{(0)} = \pm \frac{8\pi\omega}{Lc^2} \sum_{n=0} \left(1 - \frac{1}{2} \delta_{n0}\right) F_\pm(\omega, q_n), \quad (39)$$

$$Z_\pm^{(1)} = \pm \frac{8\pi\omega}{Lc^2} \sum_{n=0} \left(1 - \frac{1}{2} \delta_{n0}\right) (-1)^n F_\pm(\omega, q_n). \quad (40)$$

To get the expression for the transmission coefficient which is determined by the ratio of the amplitudes of the transmitted field (E_t) at $z=L$ and the incident field (E_i) at $z=0$, we use the Maxwell boundary conditions

$$2E_i^\pm = E_\pm(0) + b_\pm(0), \quad E_t^\pm = b_\pm(L). \quad (41)$$

Then, we define $T_\pm = |E_t^\pm / E_i^\pm|$ where $E_t^\pm / E_i^\pm = [E_\pm(L) + b_\pm(L)] / [E_\pm(0) + b_\pm(0)]$. Assuming that the transmission is small ($T_\pm \ll 1$), we get the asymptotic expression

$$\frac{E_t^\pm}{E_i^\pm} \approx \frac{c}{4\pi} Z_\pm^{(1)}, \quad (42)$$

where $Z_\pm^{(1)}$ is given by relation (40).

Therefore, keeping the “-” polarization, we can start from the following expression for the transmission coefficient:

$$T = \frac{4i\omega}{Lc} \sum_{n=0} (-1)^{n+1} \left(1 - \frac{1}{2} \delta_{n0}\right) F_-(\omega, q_n), \quad (43)$$

Using Poisson’s summation formula

$$\sum_{n=0} y(q_n) = \sum_{r=-\infty}^{\infty} \int_0^{\infty} y\left(\frac{\pi}{L}x\right) \exp(2\pi irx) dx, \quad (44)$$

we convert the expression for the transmission coefficient to the form

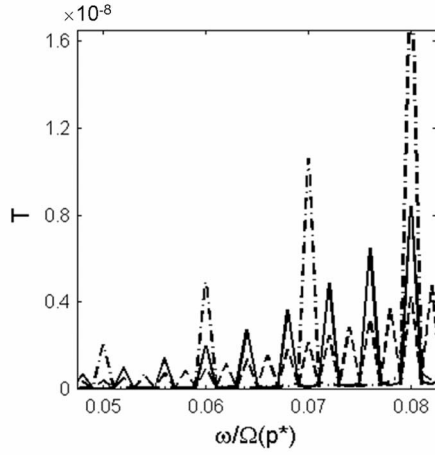


FIG. 4. Size oscillations in the transmission coefficient for the transverse electromagnetic wave traveling through a metal film which originate from the low-frequency Fermi-liquid mode. The curves are plotted at $\alpha_2 = -0.2$ and $s = 3$. $\Omega\tau \sim 50$, $\xi = 10^3$, and $L/l = 0.01$ (dash-dot line), 0.025 (solid line), and 0.05 (dashed line).

$$T = \frac{2}{\pi} \frac{\omega}{c} \int_{-\infty}^{\infty} \text{sign}(q) \csc(Lq) F_-(\omega, q) dq, \quad (45)$$

where $\text{sign}(q)$ is the sign function: $\text{sign}(q) = |q|/q$. An important contribution to the integral in Eq. (45) comes from the poles of the function $F_-(\omega, q)$, i.e., the roots of the dispersion equation [Eq. (16)] for the relevant polarization. The contribution from the considered low-frequency mode to the transmission coefficient is equal to a residue from the appropriate pole of the integrand in expression (45).

When dA/dp_z gets its extremal values at the inflection lines ($p_z = \pm p^*$), the contribution T_1 from this wave to the transmission coefficient is

$$T_1 \approx \frac{\rho_s v_0}{\xi c} \alpha_2^2 \tilde{\omega}^3 (|\alpha_2| \tilde{\omega})^{-7s/2} (1 - \tilde{\omega})^{-3/(2s-5)} \times \left\{ \sin^2 \left[\frac{L}{l} \Omega \tau (1 - \tilde{\omega}) \right] + \sinh^2 \left(\frac{L}{l} \right) \right\}^{-1/2}, \quad (46)$$

where $\tilde{\omega} = \omega/\Omega(p^*)$ and ρ_s is the dimensionless factor of the order of unity:

$$\rho_s = \frac{2s-3}{2s-5} \frac{Q_0}{Q_2} (x^*)^2 (v_s)^{(2s-3)/(2s-5)}. \quad (47)$$

The size oscillations of the transmission coefficient arising due to the low-frequency cyclotron wave could be observed in thin films whose thickness is smaller than the electron mean free path ($L \ll l$). Under this condition, we can obtain the following estimates for $|T_1|$ in a typical metal in a magnetic field of the order of 5 T and for the shape parameter $s=3$:

$$T_1 \sim (10^{-10} - 10^{-11}) l/L. \quad (48)$$

Size oscillations of the transmission coefficient described by expression (43) are shown in Figs. 4 and 5. When ($s=3$) (see Fig. 4), the oscillation amplitudes accept values $\sim 10^{-8} - 10^{-9}$

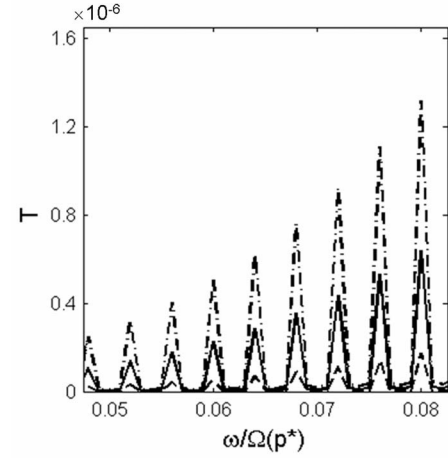


FIG. 5. The dependence of the transmission from the FS shape near the inflection line. The curves are plotted for $s=3$ (dashed line), 4 (solid line), and 5 (dash-dot line) and $L/l=0.025$. The remaining parameters coincide with those used to plot the curves in Fig. 4.

depending on the ratio L/l . The values of such order can be measured in experiments on the transmission of electromagnetic waves through thin metal films. However, the oscillation magnitudes may reach significantly greater values when the shape parameter increases. As displayed in Fig. 5, T_1 can reach the values of the order of 10^{-6} when $s=5$.

Under the considered conditions, the transmission coefficient also includes a contribution T_2 from electrons corresponding to the vicinities of those cross sections of the Fermi surface where the longitudinal component of their velocity becomes zero. This contribution always exists under the anomalous skin effect. The most favorable conditions for the observation of the size oscillations arising due to the Fermi-liquid wave in experiments are provided when $T_1 > T_2$. It happens when $L\omega\xi > v_0$. When the FS everywhere has a finite nonzero curvature the expression for T_2 can be written as follows:²⁰

$$T_2 \approx \frac{4}{3} \frac{v_0}{c} \frac{1}{\xi} \exp\left(-\frac{L\omega\tau\xi}{l}\right). \quad (49)$$

In magnetic fields $\sim 5T$ and for $L\omega \sim v_0$, the contribution T_2 has the order of $10^{-10} - 10^{-11}$, i.e., the predominance of the term T_1 over T_2 can be reached. Besides the contributions from the poles of $F_-(\omega, q)$, the transmission coefficient [Eq. (45)] includes a term T_3 originating from the branch points of this function in the q, ω complex plane. These points cause the Gantmakher-Kaner size oscillations of the transmission coefficient.²¹ However, for $L\Omega > v_0$, these oscillations have a magnitude of the order of $10^{-9} - 10^{-10}$ or less. So, the present estimates give grounds to expect that the size oscillations in the transmission coefficient of the electromagnetic wave through a thin film of a clean metal may include a rather significant or even predominating contribution, which arises due to the low-frequency ($\omega \ll \Omega$) Fermi-liquid mode.

Fermi surfaces of real metals are very complex in shape and most of them have inflection lines, so there are grounds

to expect the low-frequency Fermi-liquid waves to appear in some metals. Especially promising are such metals as cadmium, tungsten, and molybdenum where collective excitations near the Doppler-shifted cyclotron resonance (doppletrons) occur.¹²⁻¹⁴ Another kind of interesting substances are quasi-two-dimensional conductors. Applying the external magnetic field along the FS axis and using the tight-binding approximation for the charge carriers, we see that the maximum longitudinal velocity of the latter is reached at the FS inflection lines where $d^2A/dp_z^2=0$. So, we may expect the low-frequency Fermi-liquid wave to appear at some of these substances, along with the usual Fermi-liquid cyclotron wave.

IV. CONCLUSION

It is a common knowledge that electron-electron correlations in the system of conduction electrons of a metal may cause occurrences of some collective excitations (Fermi-liquid modes), whose frequencies are rather close to the cyclotron frequency at strong magnetic fields ($\Omega\tau \gg 1$). Here, we show that a Fermi-liquid wave can appear in clean metals at significantly lower frequencies ($\tau^{-1} \ll \omega \ll \Omega$). The major part in the wave formation is taken by the electrons (or holes) which move along the applied magnetic field with the maximum velocity v_0 . Usually, such electrons belong to the vicinities of limiting points or inflection lines on the FS. When the FS possesses nearly paraboloidal segments including these points for lines, the longitudinal velocity of the charge carriers slowly varies over such FS segments, remain-

ing close to its maximum value v_0 . This strengthens the response of these efficient electrons to the external disturbances. As a result, the spectrum of the Fermi-liquid cyclotron wave may be significantly changed. These changes were analyzed in some earlier works (see, e.g., Ref. 15) assuming that the cyclotron mass of the charge carriers remains the same all over the FS. Under this assumption, it was shown that the appropriate FS geometry at the segments where the maximum longitudinal velocity of electrons for holes is reached may cause the dispersion curve of the transverse Fermi-liquid cyclotron wave to be extended to the region of comparatively low frequencies ($\omega \ll \Omega$).

In the present work, we take into account the dependence of the cyclotron mass of p_z . This more realistic analysis leads to the conclusion that one may hardly expect the above extension of the Fermi-liquid cyclotron wave spectrum in real metals. However, when the FS has the suitable geometry at the segments where the charge carriers with maximum longitudinal velocity are concentrated, the low-frequency Fermi-liquid mode may occur in the metal alongside the usual Fermi-liquid cyclotron wave. This mode may cause a special kind of size oscillations in the transmission coefficient for an electromagnetic wave of the corresponding frequency and polarization incident on a thin metal film.

ACKNOWLEDGMENTS

The author thanks G. M. Zimbovsky for help with the paper. This work was supported by NSF Advance Program No. SBE-0123654, DoD Grant No. W911NF-06-1-0519, and PR Space Grant No. NGTS/40091.

¹A. A. Abrikosov, *Foundations of the Theory of Metal* (North-Holland, Amsterdam, 1988).

²P. M. Platzman and P. A. Wolff, *Waves and Interactions in Solid State Plasma* (Academic, New York, 1973).

³E. A. Kaner and V. G. Skobov, *Adv. Phys.* **17**, 605 (1968).

⁴V. P. Silin, *Zh. Eksp. Teor. Fiz.* **33**, 1227 (1958) [*Sov. Phys. JETP* **6**, 1945 (1958)].

⁵S. Schultz and G. Dunifer, *Phys. Rev. Lett.* **18**, 283 (1967).

⁶P. M. Platzman, W. Walsh, and E-Ni Foo, *Phys. Rev.* **172**, 689 (1968).

⁷Y. C. Cheng, J. S. Clarke, and D. Mermmin, *Phys. Rev. Lett.* **20**, 1486 (1968).

⁸At $q > q_m$, the wave is damped by the conduction electrons.

⁹S. C. Ying and J. J. Quinn, *Phys. Rev.* **180**, 193 (1969).

¹⁰T. P. Alodzhantz, *Zh. Eksp. Teor. Fiz.* **59**, 1429 (1970) [*Sov. Phys. JETP* **32**, 780 (1971)].

¹¹Y. C. Cheng, *Phys. Rev. B* **3**, 2987 (1971).

¹²S. V. Lavrova, V. T. Medvedev, V. G. Skobov, L. M. Fisher, and A. S. Chernov, *Zh. Eksp. Teor. Fiz.* **64**, 1839 (1973) [*Sov. Phys. JETP* **37**, 929 (1973)].

¹³V. T. Medvedev, V. G. Skobov, L. M. Fisher, and V. A. Yudin, *Zh. Eksp. Teor. Fiz.* **69**, 2267 (1975) [*Sov. Phys. JETP* **42**, 1152 (1975)].

¹⁴D. S. Folk, B. Gerson, and J. F. Carolan, *Phys. Rev. B* **1**, 406 (1970).

¹⁵N. A. Zimbovskaya, V. I. Okulov, A. Yu. Romanov, and V. P. Silin, *Fiz. Nizk. Temp.* **8**, 930 (1982) [*Sov. J. Low Temp. Phys.* **8**, 468 (1982)].

¹⁶N. A. Zimbovskaya and G. Gumbs, *Phys. Rev. B* **72**, 045112 (2005).

¹⁷O. V. Kirichenko, V. G. Peschansky, and D. I. Stepanenko, *Phys. Rev. B* **71**, 045304 (2005).

¹⁸N. A. Zimbovskaya, *Phys. Rev. B* **74**, 035110 (2006).

¹⁹N. A. Zimbovskaya, V. I. Okulov, A. Yu. Romanov, and V. P. Silin, *Fiz. Met. Metalloved.* **58**, 851 (1984).

²⁰N. A. Zimbovskaya and V. I. Okulov, *Fiz. Met. Metalloved.* **61**, 230 (1986).

²¹V. F. Gantmakher and E. A. Kaner, *Zh. Eksp. Teor. Fiz.* **48**, 1572 (1965) [*Sov. Phys. JETP* **21**, 1053 (1965)].